

OFF-MOMENTUM OPTICS AT SuperKEKB

Y. Ohnishi*, H. Koiso, A. Morita, K. Ohmi, H. Sugimoto, KEK, OHO 1-1, Tsukuba, Japan
 K. Oide, CERN, Geneva, Switzerland

Abstract

The nano-beam scheme can squeeze the vertical beta function at the IP much smaller than the bunch length. It implies that the large chromaticity is generated in the vicinity of the final focus quadrupole magnets and the strong sextupoles, for instance the local chromaticity corrections, are adopted to correct the chromaticity. While understanding of the off-momentum optics is important to optimize the dynamic aperture to make Touschek lifetime long and to reduce the luminosity degradation due to chromatic behaviors. In general, there is a discrepancy between measurements of chromaticity and those obtained from the optics model. The chromatic phase-advance is introduced to measure the off-momentum optics and correct by adjustments of sextupole magnets.

INTRODUCTION

SuperKEKB is an electron-positron double-ring collider [1] and the Belle II detector [2] built to explore new physics in the collider experiment. The physics program of the recent B-factory delivering extremely high statistics is almost independent of and complementary to the high energy experiments at the LHC. The target luminosity is $8 \times 10^{35} \text{ cm}^{-2} \text{ s}^{-1}$, which is 40 times the performance of KEKB [3] that has been operated for 11 years until 2010. The strategy for the luminosity upgrade is a nano-beam scheme. The collision of low emittance beams under a large crossing angle allows squeezing the beta functions at the IP to value much smaller than the bunch length. Consequently, extremely higher luminosity can be expected with only twice the beam current of KEKB.

The small beta functions at the IP implies that a large chromaticity is generated in the vicinity of the final focus magnets (QC1 and QC2). The natural chromaticity calculated from the lattice model in Phase 2 is shown in Table 1. Because the chromaticity generated from QC1 and QC2 is very large, we adopt local chromaticity corrections for both x and y directions. The local chromaticity correction and the arc lattice utilize non-interleaved sextupole correction scheme. Two identical sextupole magnets are connected by $-I'$ transfer matrix. A nonlinear kick from either of two sextupole magnets can be compensated by another sextupole magnets for on-momentum particles in this scheme. Therefore, a large dynamic aperture can be expected. The number of sextupole families is 54 for each ring. The field strength of the sextupole magnet is optimized to maximized the dynamic aperture or Touschek lifetime as well as adjustments of the linear chromaticity.

Figure 1 shows comparisons between typical measured chromaticity and that calculated from the model lattice. The

Table 1: Typical parameters such as the beta functions and chromaticity in Phase 2

	LER	HER	Unit
Beam Energy	4	7	GeV
β_x^*	200	100	mm
β_y^*	3	3	mm
β_x at QC2L	62.2	235.2	
β_x at QC2R	62.1	288.0	
β_y at QC1L	255.6	578.0	
β_y at QC1R	254.7	581.6	
ξ_{x0}	-69	-97	
ξ_{y0}	-146	-168	
ξ_x (QC2)	-8	-25	
ξ_y (QC1)	-67	-100	
ν_x	44.558	45.541	
ν_y	46.615	43.610	
α_p	2.88×10^{-4}	4.50×10^{-4}	

optical functions are calculated by using SAD [4] for the model lattice. There are discrepancies between the measured value and the model by $\Delta\xi_x = 1 \sim 1.5$ and $\Delta\xi_y = 2.5 \sim 3.3$ in the LER, $\Delta\xi_x = 0.5 \sim 0.7$ and $\Delta\xi_y = 3 \sim 3.3$ in the HER, which corresponds to 1~2 % deviation.

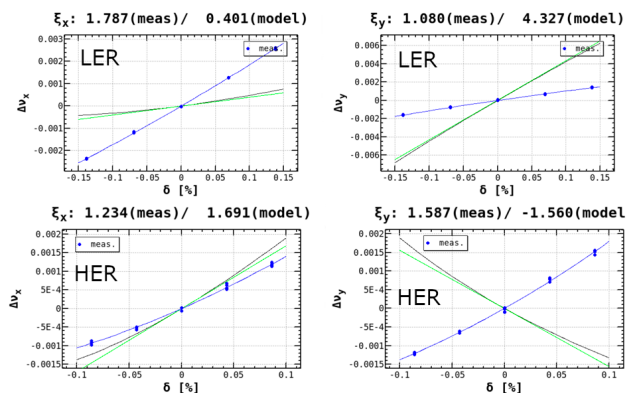


Figure 1: Chromaticity in the LER and HER, respectively. The blue plots indicate measured tune shift and black line for the model calculation. The green line show a derivative of the model tune shift at the on-momentum.

First of all, as the motivation of this article, why there is discrepancy between model and measurement? We can change the chromaticity as a relative value by using model calculations. However, the absolute value is unclear even though optics corrections have been done and worked well for corrections of beta functions and dispersions. Secondary, the off-momentum optics is necessary to understand well to

* yukiyoshi.ohnishi@kek.jp

optimize dynamic aperture. The low emittance lattice and low beta at the IP reduce dynamic aperture and Touschek lifetime becomes an issue for both linac injector capability although a top-up injection and detector backgrounds.

MEASUREMENT AND CORRECTION OF CHROMATIC PHASE ADVANCE

The beta function and phase advance are measured by close orbit distortions induced by dipole corrector magnets [5]. The close orbit is written by

$$\Delta x_i^j = \frac{\Delta \theta_j}{2 \sin(\pi \nu)} \sqrt{\beta_i \beta_j} \cos(|\psi_i - \psi_j| - \pi \nu) \quad (1)$$

$$= A_j \{C_j(C_i \cos \pi \nu + a_{ij} S_i \sin \pi \nu) \quad (2)$$

$$+ S_j(S_i \cos \pi \nu - a_{ij} C_i \sin \pi \nu)\}, \quad (3)$$

where

$$A_j = \frac{\Delta \theta_j}{2 \sin \pi \nu} \quad (4)$$

$$C_{i,j} = \sqrt{\beta_{i,j}} \cos \psi_{i,j} \quad (5)$$

$$S_{i,j} = \sqrt{\beta_{i,j}} \sin \psi_{i,j} \quad (6)$$

$$a_{ij} = \text{sign}(\psi_i - \psi_j). \quad (7)$$

The fitting parameters are A_j , $C_{i,j}$, and $S_{i,j}$, for i th BPM from 1 to N and j th dipole corrector from 1 to M . These equations can be solved by a least-square fitting with a minimization of

$$X^2 = \sum_{i,j}^{N,M} (\Delta x_i^j - \Delta x_{i,meas.}^j)^2 \quad (8)$$

$$\sum_{i=1}^N \frac{1}{\beta_i} = \sum_{i=1}^N \frac{1}{\beta_{i,design}}, \quad (9)$$

when $N \times M > 2(M + N)$ is satisfied. the number of BPMs is about 450 for each ring and six different kinds of dipole correctors are used to induce closed orbit distortions.

The chromatic phase-advance in the horizontal and the vertical direction are expressed as

$$\chi_i(w) = \frac{1}{2\pi} \frac{\partial \Delta \psi_{w,i}}{\partial \delta}, \quad (10)$$

where

$$\Delta \psi_{w,i} = \psi_{w,i} - \psi_{w,i-1}, \quad (11)$$

and w stands for x or y . The number of locations is about 450 for each ring which corresponds to the neighboring BPMs. In order to correct the chromatic phase-advance, the field gradient of the sextupole magnets, ΔK_2 , are obtained

by solving these equations:

$$\begin{pmatrix} \chi_{1,m}(x) - \chi_{1,d}(x) \\ \vdots \\ \chi_{N,m}(x) - \chi_{N,d}(x) \\ \chi_{1,m}(y) - \chi_{1,d}(y) \\ \vdots \\ \chi_{N,m}(y) - \chi_{N,d}(y) \\ \xi_{x,m} - \xi_{x,d} \\ \xi_{y,m} - \xi_{y,d} \end{pmatrix} = M_{resp} \begin{pmatrix} \Delta K_{2,1}/K_{2,1} \\ \Delta K_{2,2}/K_{2,2} \\ \vdots \\ \Delta K_{2,M}/K_{2,M} \end{pmatrix}, \quad (12)$$

where m indicates the measurements, d indicates the model calculation, M_{resp} is a response matrix calculated by the model lattice, N is the number of BPMs, and M is the number of families of the sextupole magnets, M is 54. These equations are solved by using a singular value decomposition (SVD). The phase advance for each momentum deviations are measured with the frequency shift between -250 Hz and +250 Hz for 5 different momentum deviations. The rf frequency is 509 MHz, then the momentum deviation is calculated with the momentum compaction, α_p , which is shown in Table 1. The corrections for the sextupole families in the LER are shown in Fig. 2. The field gradient, K_2 , which corresponds to the rated current for the defocusing sextupole(SD) is -8.2 1/m² and 5.0 1/m² for the focusing sextupole(SF). The amount of the sextupole correction is within 7 % of the rated current.

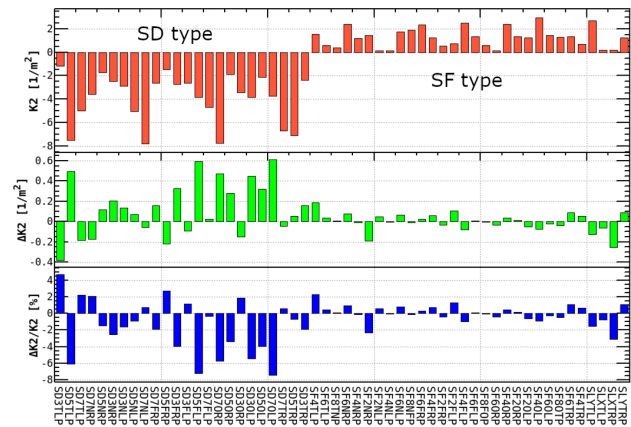


Figure 2: Correction for the field gradient of the sextupole magnet families in the LER.

Figure 3 shows the chromatic phase-advance before the correction, on the other hand, that after the correction shown in Fig. 4 in the LER. The blue plots indicate the measured values and the green plots indicate the model calculations. In the vertical direction, there are still discrepancies after the correction between the measurement and model in the vicinity of the final focus system. This implies there is a local chromaticity source in the final focus, the sextupole magnets in the arc lattice and the local chromaticity correction can not correct this chromatic effect. Since sextupole corrector coils are installed in the final focus system, we expect that there is a feasibility of the local correction.

The chromaticity before and after the correction is shown in Fig. 5. The comparison of chromaticity before and after the correction is shown in Table 2. The chromaticity in the model lattice is also corrected to the measurement by the correction of chromatic phase-advance.

Table 2: Chromaticity before and after correction in the LER

	Meas.	Model before	Model after
ξ_x	1.97	1.04	2.01
ξ_y	-2.15	2.62	-1.66

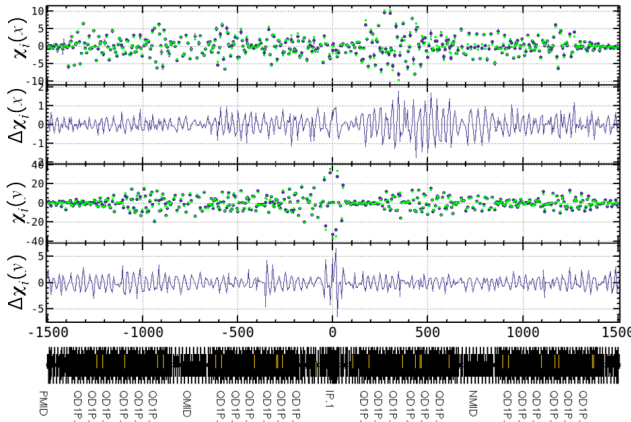


Figure 3: Chromatic phase-advance before correction in the LER.

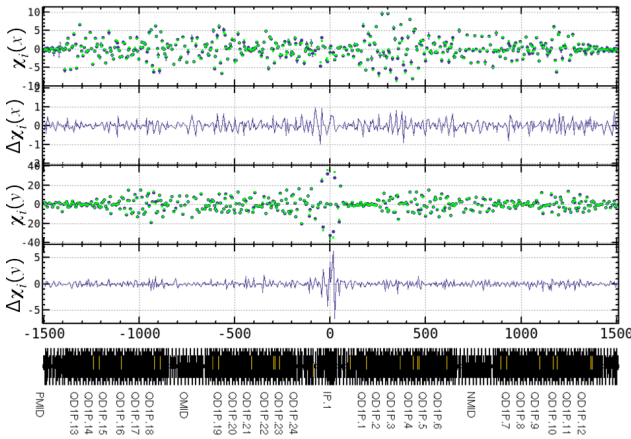


Figure 4: Chromatic phase-advance after correction in the LER.

MEASUREMENT OF CHROMATIC XY COUPLING

The interaction region is very complicated at SuperKEKB because of the final focus magnets inside the solenoid field generated by Belle II detector and anti-solenoid to compensate the detector solenoid field of 1.5 T as much as possible.

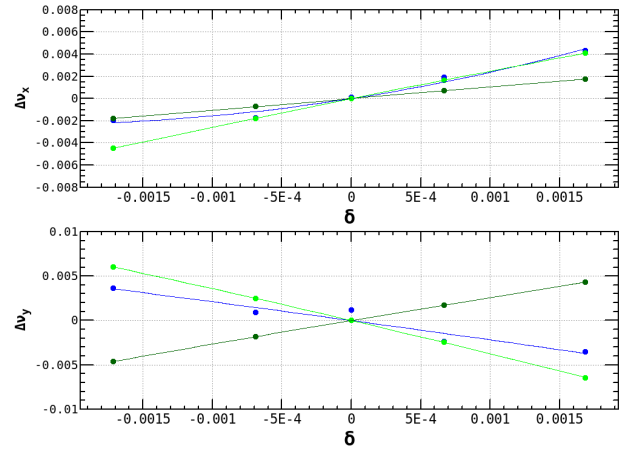


Figure 5: Chromaticity in the LER. The blue plots indicate measured values. The dark green plots indicate before correction and the green plots indicate after correction.

Furthermore, the final focus magnet has a slant angle against the solenoid axis by the half of crossing angle and the position of the magnet is shifted on the xy plane for each QC1s and QC2s. Although the XY couplings at the IP is zero in the model lattice, chromatic XY couplings are finite values which can be corrected by using skew sextupole magnets in principle.

The relationship between a physical coordinate and decoupled coordinate system of a particle is written by

$$\begin{pmatrix} x \\ p_x \\ y \\ p_y \end{pmatrix} = \begin{pmatrix} \mu & 0 & r_4 & -r_2 \\ 0 & \mu & -r_3 & r_1 \\ -r_1 & -r_2 & \mu & 0 \\ -r_3 & -r_4 & 0 & \mu \end{pmatrix} \begin{pmatrix} u \\ p_u \\ v \\ p_v \end{pmatrix}, \quad (13)$$

where (x, p_x, y, p_y) is the physical coordinate system, (u, p_u, v, p_v) is the decoupled coordinate system, $r_1 \sim r_4$ are the XY coupling parameters, and $\mu^2 + (r_1 r_3 - r_2 r_4) = 1$. The XY coupling parameter is defined at each point along the beam orbit. When only one mode is excited, the phase space of the beam accompanied with a betatron oscillation in the physical coordinate can be obtained by $v = 0$ and $p_v = 0$ for the H-mode, on the other hand $u = 0$ and $p_u = 0$ for the V-mode, respectively. In the case of H-mode, the XY coupling parameters are derived by

$$\begin{pmatrix} r_1 & r_3 \\ r_2 & r_4 \end{pmatrix} = -\mu \Sigma^{-1} \begin{pmatrix} \langle xy \rangle & \langle xp_y \rangle \\ \langle px_y \rangle & \langle px_p_y \rangle \end{pmatrix}, \quad (14)$$

where

$$\Sigma = \begin{pmatrix} \langle x^2 \rangle & \langle xp_x \rangle \\ \langle xp_x \rangle & \langle p_x^2 \rangle \end{pmatrix}. \quad (15)$$

The beam orbit for the betatron oscillation can be measured by Turn-by-Turn BPMs (TbT BPMs) [6]. Here, the betatron oscillation in the horizontal plane is induced by an injection kicker. The beam centroid position on two orthogonal coordinates is estimated by two TbT BPMs, which are located

Content from this work may be used under the terms of the CC BY 3.0 licence (© 2018). Any distribution of this work must maintain attribution to the author(s), title of the work, publisher, and DOI.

either side of the IP near the final focus magnets (QC1 and QC2). The betatron oscillations, which determine the decoupled coordinate by utilizing tune frequency, are extracted by FFT analysis. Therefore, the rotation of injection kicker can be distinguished from the XY couplings, however, it is difficult to separate the rotation of TbT BPMs and the XY couplings. Assuming the transfer matrix of the model lattice, we can reconstruct the phase space at the IP. The momentum is shifted by changing the rf frequency to measure the chromatic XY couplings with the momentum deviation. The 5 different frequency shifts from -200 Hz to +200 Hz are utilized.

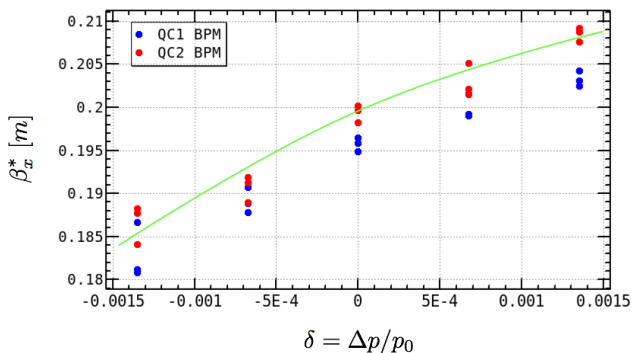


Figure 6: Chromatic horizontal beta function at the IP in the LER. The blue plots indicates the values obtained from QC1 and the red plots from QC2.

When the phase space of x and p_x is considered, the horizontal beta function at the IP can be obtained. Figure 6 shows the horizontal beta function at the IP as a function of the momentum deviation in the LER, namely the chromatic beta function. The chromatic beta function at the IP is $(\partial\beta_x^*/\partial\delta)/\beta_x^* = 50$ in the figure.

The chromatic XY coupling parameters at the IP measured by TbT BPMs in the LER are shown in Fig. 7. The absolute value of XY coupling, r_4^* , is different between QC1 and QC2 BPM but $r_1^* \sim r_3^*$ are consistent with each other. The chromatic XY couplings obtained from QC1 and QC2 BPMs are almost same results.

SUMMARY

The analysis of off-momentum optics has been performed. Understanding of the off-momentum optics is necessary not only to optimize a dynamic aperture but also to improve

luminosity performance [7]. Measurements of the chromatic phase-advance and the correction by using adjustment of field gradient for the sextupole magnets are presented. The correction of the sextupole magnets is less than 7 % of the rated current. Consequently, the chromatic phase-advance and chromaticity can be corrected on the model lattice. There is a residual between measurements and the model for the chromatic phase-advance in the vicinity of the final focus magnets. This behavior causes there is sextupole error field in the final focus magnets which has sextupole corrector coils.

The chromatic XY couplings at the IP are also measured by using TbT BPMs. In order to reconstruct the phase space, two TbT BPMs are utilized with assuming the transfer matrix of the model lattice. The r_3^* and r_4^* can be measured, however, r_1^* and r_2^* are difficult to measure absolute values due to an accuracy of the BPM resolution. The leakage amplitude of the beam position in the vertical plane from the horizontal oscillation is very small since the phase advance between the QC1 BPM and the IP is almost $\pi/2$. The relative change for the momentum deviation can be observed. The chromatic XY couplings at the IP is almost flat except for r_3^* and $r_3'^*$ is measured to be -470 in the LER.

ACKNOWLEDGMENT

This work was supported by JSPS KAKENHI Grant Number 17K05475.

REFERENCES

- [1] Y. Ohnishi *et al.*, "Accelerator design at SuperKEKB", *Prog. Theor. Exp. Phys.*, vol. 2013, no. 3, p. 03A011, Mar. 2013, <https://doi.org/10.1093/ptep/pts083>
- [2] Belle II Technical Design Report, <http://arXiv.org/abs/1011.0352>
- [3] T. Abe *et al.*, "Achievements of KEKB", *Prog. Theor. Exp. Phys.*, vol. 2013, no. 3, p. 03A001, Mar. 2013, <https://doi.org/10.1093/ptep/pts102>
- [4] *Strategic Accelerator Design*, <http://acc-physics.kek.jp/SAD>
- [5] A. Morita *et al.*, presented at eeFACT2018, Hong Kong, China, September 2018, paper TUOAB04, this conference.
- [6] Y. Ohnishi *et al.*, "Measurement of chromatic X-Y coupling", *Phys. Rev. SP-AB*, **12**, 091002 (2009).
- [7] K. Ohmi *et al.*, presented at eeFACT2018, Hong Kong, China, September 2018, paper TUOBB01, this conference.

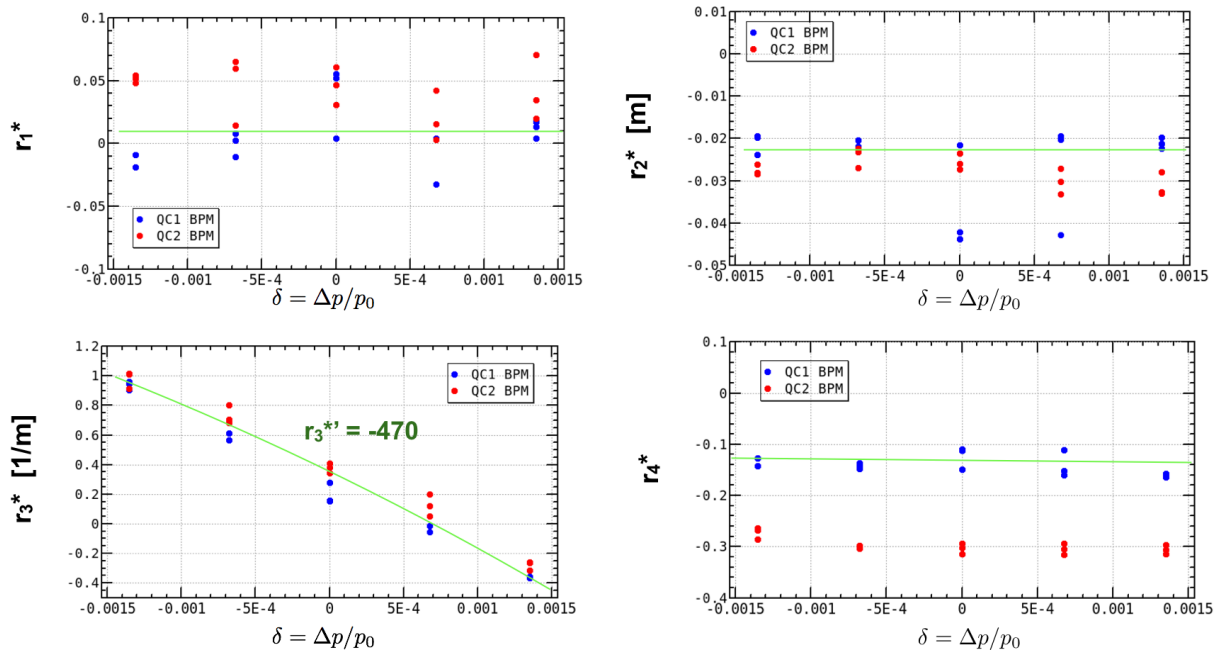


Figure 7: Chromatic XY coupling at the IP in the LER. The blue plots indicates the values obtained from QC1 and the red plots from QC2.